Title	High dynamic range image processing for non-destructive-testing
Authors(s)	Ghosh, Bidisha, Pakrashi, Vikram, Schoefs, Franck
Publication date	2011-10-17
Publication information	Ghosh, Bidisha, Vikram Pakrashi, and Franck Schoefs. “High Dynamic Range Image Processing for Non-Destructive-Testing” 15, no. 7 (October 17, 2011).
Publisher	Taylor & Francis
Item record/more information	http://hdl.handle.net/10197/10454
Publisher's statement	This is an Accepted Manuscript of an article published by Taylor & Francis in European Journal of Environmental and Civil Engineering on 17 October 2011, available online: http://www.tandfonline.com/10.1080/19648189.2011.9695295.
Publisher's version (DOI)	10.3166/EJECE.15.1085-1096

High Dynamic Range Image Processing for Structural Health Monitoring

Bidisha Ghosh* — Vikram Pakrashi — Franck Schoefs*****

**Department of Civil, Structural and Environmental Engineering*
Trinity College Dublin
Dublin 2
IRELAND

bghosh@tcd.ie

***Roughan & O'Donovan Consulting Engineers*
Arena House, Arena Road, Sandyford
Dublin 18
IRELAND

pakrashv@tcd.ie

****Département de Physique*
Université de Nantes, Nantes
FRANCE

Franck.Schoefs@univ-nantes.fr

ABSTRACT. *This paper proposes High Dynamic Range (HDR) imaging as a protocol for structural health monitoring for the first time. HDR imaging protocol has been experimentally validated on images of pitting corrosion in this paper and has been further applied to isolate a range of image backgrounds that arise out of a number of environmental conditions. The superiority of HDR imaging over a standard imaging process has been demonstrated. The results indicate that the proposed protocol is not limited by the examples considered in this paper and can readily be applied to a number of infrastructure maintenance management related applications. The protocol complements and improves standard visual inspection techniques and expert opinions. This approach immediately lends itself to further mathematical and statistical analyses, both qualitative and quantitative.*

KEY WORDS :*High Dynamic Range (HDR) Imaging, Structural Health Monitoring (SHM), Pitting Corrosion, Damage Detection, Image Processing*

1. Introduction

A four step process is usually popular in the field of Structural Health Monitoring (SHM) and damage detection (Rytter 93). The first three steps are connected and involve the detection of the presence, the location and the severity of damage, while the fourth step, related to the prediction of service life is usually a separate problem by itself. In most of the world infrastructure systems or parts of the systems are continuously ageing and deteriorating. This in conjunction with limited government and private funding emphasizes the importance of infrastructure maintenance management and prioritisation through SHM (Žnidarič *et al*., 2005) Intrusive, non-intrusive and semi – intrusive testing are often carried out following visual inspections. The test results can be readily fed into Bridge Management Systems (BMS) or Infrastructure Management Systems (IMS). This approach is not specific to particular management processes for infrastructure networks and can be used to significantly affect decision making procedures and financing for infrastructure owners, managers and end users. Decision making based on testing even accommodates a more modern infrastructure specific probabilistic hierarchical approach (Pakrashi *et al*., 2005).

Among the various methods of testing, non – intrusive or Non Destructive Testing (NDT) affects the tested structure to a minimum level. The quality of results and the cost efficiency of such methods are extremely important as they directly affect the performance indices of a structure or a network of structures in terms of safety and durability at a given time. The methodology and the protocol of NDT directly relate to the quality and the quantity of transfer of benefits of an infrastructure system to the end user.

A typical and specific application in this regard can be found in the field of corroding infrastructure systems, in particular underwater marine structures undergoing pitting or any other form of corrosion. These structures often require underwater inspections and are carried out by trained divers who usually are not structural experts (Rouhan *et al*., 2003). Traditionally, photographic and video recordings are available from diving campaigns. Descriptive and expert ranking based classification of damages are standard outputs from these data. Even when more detailed surveys and experiments are carried out, only pointwise information is generally available (Boukinda *et al*., 2007).

Though a natural choice, the use of image processing in classifying damage conditions has not been used to the potential it holds and no testing protocol currently exists. Image processing based detection of pitting corrosion, although reported in literature (Itzhak *et al*., 1981; Choi *et al*., 2005) , has not received significant attention and the quality of detection obtained as a function of image conditions has been barely looked into (Pakrashi *et al*., 2010). It is felt by the authors, that image processing based detection of corrosion can be significantly improved for a wide range of problems through the specification of certain protocols. Such protocols give rise to a number of opportunities well beyond standardising and homogenising test methods and the comparison of test results under varying environmental conditions.

The specification of an improved imaging protocol partially offsets the inexperience or the lack of expertise on the part of the diver and enhances the quality of input data to the analysing engineer, scientist or expert. The significant increase of the quality of the input data without the requirement of additional costs in terms of sensors or the training of individuals is extremely important. In addition, an image based approach can make a significant amount of archived image and video data available from previous inspections over a number of decades useful through correct specifications. Image processing based output data readily lends itself to mathematical and statistical treatments and the quantification of output results are significantly more correct, detailed and sophisticated. All of these advantages greatly improve the credibility of the assessment of a structure at a given time and the evolution of a structure over a period of time.

This paper proposes High Dynamic Range (HDR) imaging as a protocol for NDT based SHM. HDR imaging involves merging of a number of photographs of the same object taken at various different exposures (Battiato *et al.*, 2003). The method is quick, can be performed with a standard digital camera, requires no new sensor and demands little training or experience from the individual logging the data. HDR imaging is particularly useful for targets that are relatively static over the period of time during which the photograph is taken (Jacobs *et al.*, 2008). HDR has been successfully applied to other fields and applications, ranging from bioengineering (Wandell *et al.*, 2002) to art (Colbert *et al.*, 2005) and photography (Pell 09) to dramatically improve the quality of an image with relatively little extra effort.

To the authors' best knowledge, there has been no application of HDR imaging for SHM although it holds exceptional potential to do so. This paper applies the proposed HDR imaging protocol successfully on a number of images of steel piles belonging to on-pile wharves corroding in the spray zone of a marine environment. The involvement of expert opinions in such detections is discussed. The paper also investigates the identification and classifications of the image backgrounds. This adds a relatively new possibility to the standard four step SHM method where identification of the type of damage as well as the presence, the location and the severity is possible.

2. High Dynamic Range (HDR) Image Processing

The dynamic range of a real-world scene is the ratio between the radiance values of the brightest and the darkest parts of the scene, whereas for a display the dynamic range is the ratio between the maximum and the minimum intensities emitted from the displayed image (Reinhard *et al.*, 2005). In real world every scene has a significant amount of brightness variation (Figure 1). The human eye is capable of handling a dynamic range of 100000:1. In simpler words, the human eye can accommodate the dynamic range between the shadowy interior of a room to the sunlit views outside the window. In contrast, a typical video camera or a digital still camera provides a dynamic range of 1000:1. Hence, photographers have to decide on a limited range of radiance values which can be captured within the limited dynamic range of the camera. Any object with radiance values above or below this camera-specific dynamic range will be captured as having the maximum or minimum limiting radiance values of the specified range respectively. As a result any real world scenes with shiny metals, sun, artificial light sources or shadowy details will pose a problem to the photographer. In these cases, the captured images will be either too dark in some areas or too bright in some.

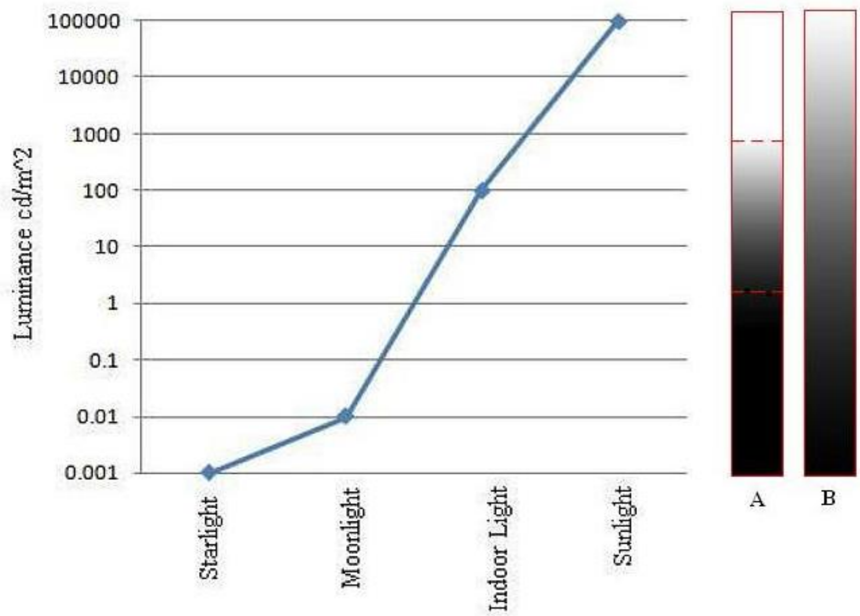

Figure **1.** *Dynamic range of nature.*

Figure 1 illustrates this point. The column (A) shows the original dynamic range of a real-world scene and column (B) shows the same captured by a conventional digital or still camera. The actual dynamic range of the camera is shown between the dotted lines in column (B).

As a result, in image-processing based SHM we are often left with photographs of significantly compromised quality for interpretation and detection purposes. The low range of brightness information of these images poses a severe limitation on what computational vision can accomplish. A very simple modification, HDR imaging, can be made to any conventional imaging system to dramatically increase this range.

An HDR image is such an image whose dynamic range exceeds the dynamic range of the capturing or the display device and in turn provides more information on every pixel of the image. The HDR images with composite radiance map can be created by taking multiple photographs of the same scene with different exposures of using a standard digital camera (Debevec *et al*., 1997). By using multiple exposure time each photograph in the sequence will have some pixels of the image properly exposed, and other pixels will be either too dark (underexposed) or too bright (overexposed). For example, a photograph captured with a long exposure time will be overexposed in the bright areas but will capture the details of the dark regions very well. A small exposure time will ensure that the details in the bright regions are captured well, but the photograph will be void of any details in the shadowy regions. The complementary nature of these images allows one to combine multiple photographs into a single, high dynamic range image whose pixel values are proportional to the true radiance values of the original scene.

3. High Dynamic Range (HDR) Image Processing

Of the many different types of damages that significantly affect structures, pitting corrosion is a specific problem where HDR imaging can be used successfully. This is a commercially important problem as it not only affects a very wide range of civil engineering structures, including piles (Liang *et al*., 2005), bridges (Darmawan *et al*., 2007) and pipes (Shivaraj *et al*., 2008) but also a range of fields as varied as from aviation (Qingyuan *et al*., 2006) to the printing industry (Sailer 07). Pitting corrosion usually creates isolated corroded units within metal and is typically characterised by their rapid change in depth over a relatively short geometric spread. Pitting corrosion is also, very typically, associated with considerable change in colour with respect to the original metal background due to the chemical reactions that bring about the corrosion (Tsushima *et al*., 1997). Detection from the typical discolouration and contrast with the background surface is generally carried out using photographs. The HDR imaging protocol assimilates the ability of human eye to detect a broader dynamic range and enhances the capacity of detection.

For the purposes of illustration, we consider photographs of steel piles belonging to on-pile wharves corroding in the spray zone of a marine environment of the Atlantic Coast, Estuary of river Loire, France. In these photographs a wide dynamic range has to be accommodated as steel may have a shiny metallic surface. Pitting corrosion occurs on the steel surface over isolated regions and is often of contrasting colour with respect to the background. Three images of the same corroding area undergoing pitting corrosion are captured with a standard commercially available digital camera (‘Bridge’ digital camera, 9.1 Megapixels (maximum: 3456 x 2592 pixels, sensitivity ISO 80 to 3200, Shutter speed: 30 - 1/4000 sec, opening: 2.8 - 5.2, focal length (KB): 28 - 560). One of these images is normally exposed, the second one is overexposed and the third one is underexposed. The amount of over and under exposure is set to one f-stop where the f-stop is defined as the ratio of the focal length of the lens to the diameter of the aperture of the lens. The three photographs are combined together to generate the HDR image following the algorithm developed by Debevec and Malik (1997). The algorithm considers multiple images of the same scene with different exposure times. These multiple images are used to recover the response function of the digital camera used to capture the photographs. The response function maps the actual quantity of light impinging on each element of the sensor array in the camera to the pixel values that the camera outputs. With the recovered response function the algorithm fuses multiple input images to a single HDR radiance map whose pixel values are proportional to the true radiance values in the scene. Figure 2 shows the HDR image along with the three parent images. The use of a higher number of parent images, above and below the normal exposure can improve the final quality of the HDR image. However, this requirement is case-specific and for the present situation three images were found to be sufficient to demonstrate the effectiveness of an HDR image.

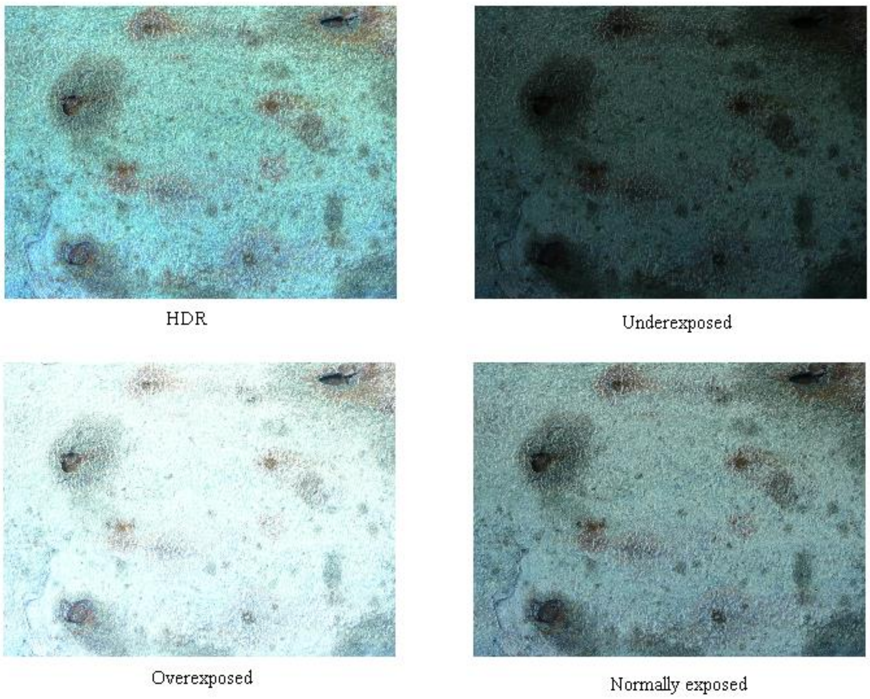

Figure **2.** *The generation of a High Dynamic Range (HDR) image.*

A line is chosen over a section of the HDR image straddling both the corroded and the uncorroded regions and the variation of Red (R), Blue (B) and Green (G) coordinates of the pixel values on that line are observed and compared with the pixel values (RGB) of the same line drawn over a normally exposed image. This comparison is presented in Figure 3. The horizontal axis refers to the local pixel coordinates on the chosen straight line along its direction on the image. The vertical axis is the axis of RGB values ranging from 0 to 256. An RGB triplet (0,0,0) refers to a completely black pixel while (256,256,256) is a perfectly white pixel. In Figure 3, the corroded zone exists from pixel 150 to about 300. The normally exposed image consists of a significant number of points with low RGB values, especially within the corroded region. This is because the corroded zone is too dark and the radiance values are outside the camera-specific dynamic range. The relative darkness within the corroded zone strips the image with normal exposure of a significant amount of information or detail that could have been observed with naked eye given the exact same lighting conditions. On the other hand, it is clearly observed that the tonal range of the HDR image is wider than that of a normally exposed image. Additionally, in HDR, a general shift of the pixel values is observed towards the higher side, the colour variations within the corroded zones are better exposed and the difference between the corroded and the uncorroded zone is fully exploited. Similar exercises have been carried out on underexposed and overexposed photographs against the HDR image. On each occasion, the HDR image was observed to be of superior quality based on the information retained. These exercises are not separately presented to avoid repetitive results.

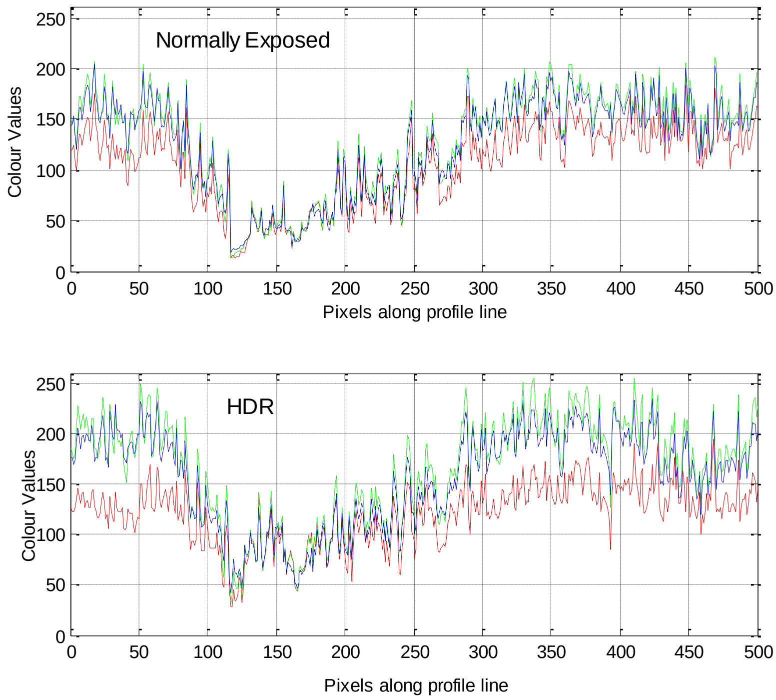

Figure **3.** *The increased tonal range during corrosion detection for an HDR image as compared to an image with normal exposure.*

It is observed in Figure 3 that the RGB values comprise of a trend and some relative high frequency fluctuations, quite akin to noise. Since the detection is dependent relatively more on the trend patterns than that of the fluctuations, a wavelet based denoising (Misiti *et al*., 2008) has been carried out on each of these pixel plots of RGB values. Figure 4 plots these pixel value trends for the normally exposed and the HDR image simultaneously.

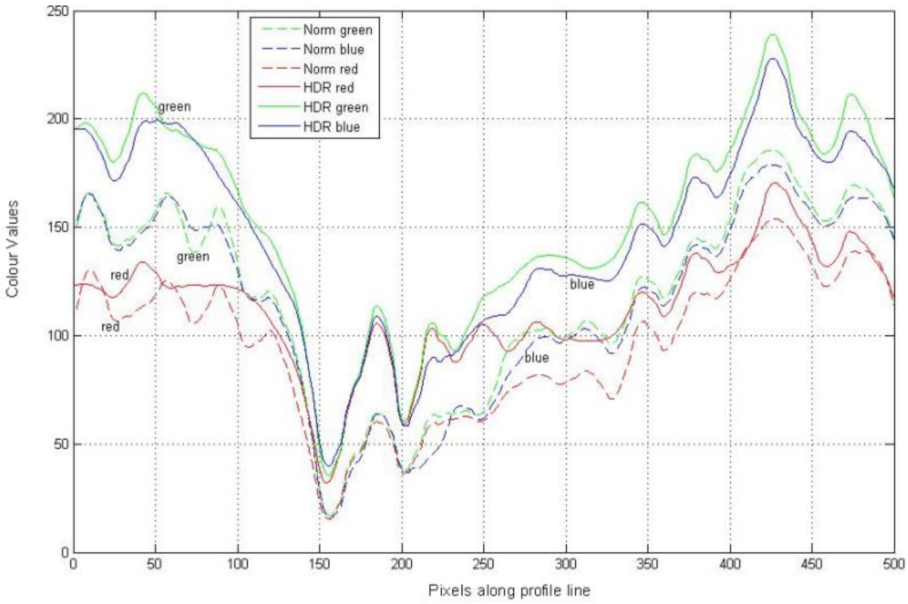

Figure **4.** *RGB trend values for HDR image in a corrosion detection scenario as compared to an image with normal exposure.*

The increased tonal range and the relatively superior information content of the HDR image are quite apparent. Consequently, a wavelet based denoising or any kind of denoising of a similar nature is proposed as a post-processing for similar detection or identification processes. It should be noted, that Red, Blue and Green pixel values are linearly combined to produce various colours and the variation of tonal range will depend on their relative participation to produce a certain colour. This explains the relatively less variation of Red in Figure 4.

The variation of the RGB pixel values along a certain line on an HDR image straddling zones of contrast is further explored for corroded steel samples featuring marine growth and dusty condition respectively. Figure 5 shows the RGB plot over linear sections with and without marine growth. The sensitivity of the values to changing situations is apparent. Figure 6 shows an image with dusty conditions. This is a particularly interesting case where staining due to corrosion occurs and can be expected to be picked up through the difference of colour intensities. On the other hand, dusty pitting zones exist where the difference of colour intensities within the zone of pitting may not be the guiding factor for detection. The pitting zone can be detected at its edges since the depth of the corroded is represented as a sudden change in relative darkness or brightness with respect to the prevailing background. A linear section is chosen in Figure 6 straddling both the stained and the unstained part. The corresponding RGB values of the pixels are observed to have changed significantly when the line enters the stained zone at around pixel values 400 to 500. The RGB values of the pixels, where the chosen line straddles the corroded and the uncorroded zone with similar backgrounds are observed to be significantly changing pointwise at the entry and at the exit locations near to pixel values 100 and 200 respectively.

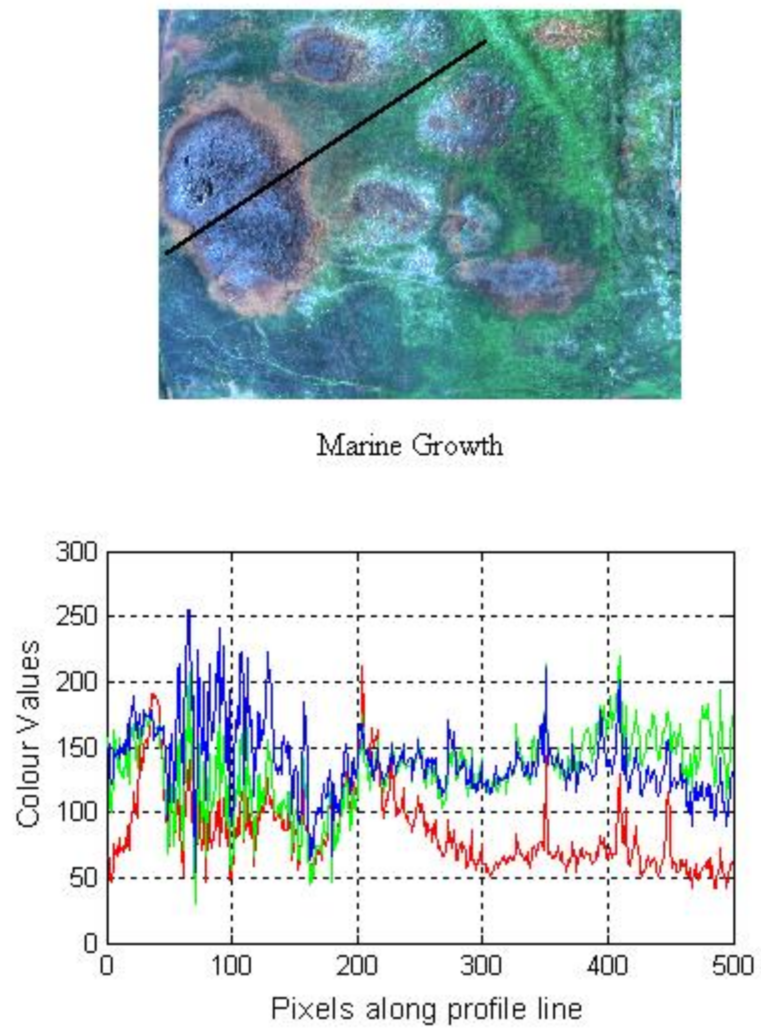

Figure **5.** *RGB values for an HDR image on a corroding specimen with marine growth.*

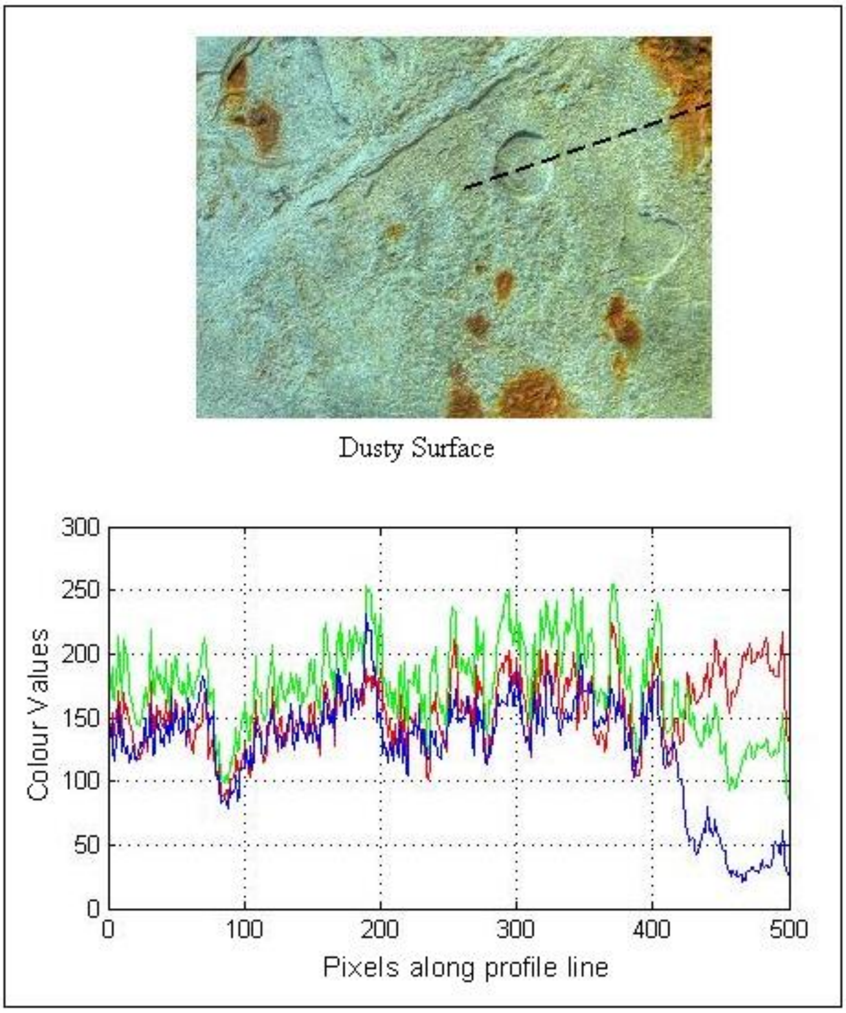

Figure **6.** *RGB values for an HDR image on a corroding specimen with dusty background.*

4. HDR Imaging Protocol for Image Background Characterisation

It is observed in the previous section, that the variation of the RGB triplet is sensitive to the type of surface that is being photographed. It is often quite an important problem to identify the kind of surface background that is present. Identification of a surface background can be traditionally and correctly carried out by experts through visual inspection. However, it would be of significant use if expert opinion on a range of visual observations can be used as an initial classifier to characterise various backgrounds automatically. If disparate image backgrounds of engineering interest readily form well-distinguishable and relatively non-overlapping clusters while similar image backgrounds relatively coagulate within a three dimensional RGB space, such a classification will be deemed feasible and applicable to real problems. A somewhat similar approach has been applied before in the field of natural image processing (Naccari *et al*., 2005).

For this purpose several realisations were carried out for a number of similar and dissimilar image backgrounds from the specimens and a three dimensional scatter plot for the RGB values were observed. Figure 7 depicts one such realisation. The RGB triplet of each pixel is represented as a point in this three dimensional space. Two of the chosen backgrounds represent the normal steel surface, but are chosen from different regions and varying texture while three other backgrounds consist of dust, marine growth and staining due to corrosion. It is seen that the disparate backgrounds form a well-defined dense non-overlapping cluster within the RGB space while the similar backgrounds of non-corroded steel form a single cluster. It is also important to note, that the dusty background is significantly separated from the non-corroded steel background and does not overlap with it even though they can appear visually similar on a photograph. The opinions of experts can be used as an initial interpretation and classification of the backgrounds and a comprehensive database can then be used to quantify these zones. In the absence of a more comprehensive set of field data, the authors do not attempt to quantify the exact zones associated with a certain degree of confidence. However, the clusters formed in Figure 7 can readily be used as a guideline. Table 1 has been inserted in this regard.

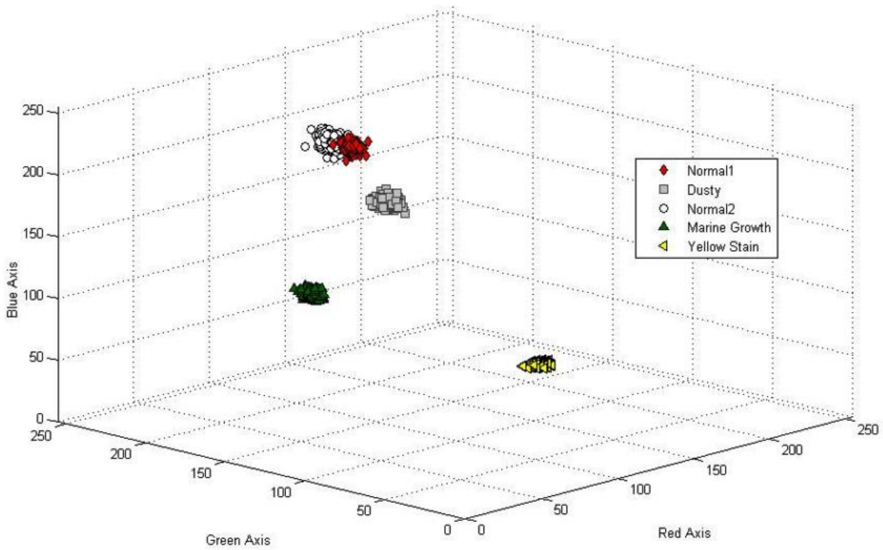

Figure **7.** *Clustering of RGB triplets based on background characterisation.*

The statistical properties of the RGB triplets are presented in Figure 8 as a Boxplot (McGill *et al*., 1978).

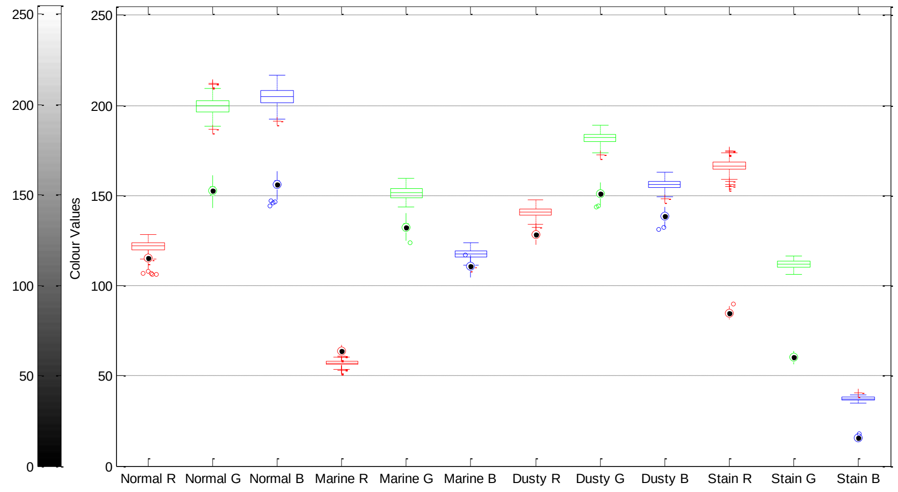

Figure **8.** *Boxplots for RGB triplet values for a number of background conditions comparing HDR image based calibrations with images of normal exposure.*

Image		Red	Green	Blue
		Pixel Values		
Normal1	**Mean**	115.18691	180.6247	208.14959
Normal1	**Std. Deviation**	25.192471	38.907286	42.05666
Normal2	**Mean**	121.5794	199.23469	204.39778
Normal2	**Std. Deviation**	38.930454	63.322038	64.227497
Marine Growth	**Mean**	57.009939	150.54289	117.64289
Marine Growth	**Std. Deviation**	18.406455	47.59369	37.035313
Dusty	**Mean**	140.905	181.85893	155.97881
Dusty	**Std. Deviation**	36.611109	46.881628	40.687193
Yellow Stain	**Mean**	166.15689	111.90803	37.348712
Yellow Stain	**Std. Deviation**	39.849552	30.307471	13.377709

Table **1.** *Cluster RGB values for various image backgrounds.*

In the figure, the boxes display the median, the extremes and the quartiles in a compact way. For the purpose of comparison, the boxes for the image with HDR exposure are plotted in the standard fashion where the horizontal line within a box depicts the median value while the crosses at the ends denote the extrema. The boxes for the normally exposed image are plotted compactly, where a black dot within a circle represents the median value and the extrema are plotted at the ends. Figure 8 emphasizes the effectiveness of the methodology proposed in this paper and demonstrates how readily various surface characterisations are possible through standard statistical analysis. The values of RGB triplets from HDR image is consistently higher than that of a normally exposed image and the calibrated values for various image backgrounds are non- overlapping. Consequently, for a wide number of interpretative classes of image situations the proposed protocol is readily applicable.

5. Discussion and Conclusion

This paper proposes High Dynamic Range (HDR) imaging as a protocol for image processing based damage detection and Structural Health Monitoring (SHM). HDR images can capture a wide range of radiance values providing details in dark and bright, damaged and undamaged surfaces. The increased tonal range and colour value information content of HDR image over a regular photograph has been shown. HDR imaging requires no extra sensor and very little training on the part of the user but provides significantly more information than a standard imaging. The image characterisation of a number of various backgrounds, including pitting corrosion has been successfully carried out on steel specimens undergoing corrosion within a marine environment.

The proposed protocol can be applied to a range of problems and is expected to play a significant role in the specification of loads on underwater structures due to marine growth. The methodology shown in this paper can accommodate a wide array of photographic and video records from archives and provide useful information from them that can readily be used for infrastructure maintenance and management over a long period of time.

Acknowledgement: *DURATINET (Durable Transport Infrastructures in the Atlantic Area Network) project, nr 2008-1/049, approved by the "Atlantic Area Transnational Program 2007-2013" and co-financed by the ERDF.*

References

Rytter A., *Interfaces homme machine*, Paris, Hermès, 1997.

Demeure I., Farhat J., "Systèmes de processus légers: concepts et exemples", *Technique et Science Informatiques*, vol. 13 no. 6, 1994, p. 765-795.

Lallouet A., “DP-LOG: un langage logique data-parallèle”, *Actes des 6 journées francophones de programmation logique et programmation par contraintes JFPLC’97,* Orléans, 26-28 mai 1997, Paris, Hermès, p. 53-68.

Braun T., Diot C., Hoglander A., Roca V., An experimental user level of implementation of TCP, rapport de recherche no. 265. septembre 1995, INRIA.

Rytter A. *Vibration based inspection of civil engineering structures*. PhD Thesis, Aalborg University, Denmark; 1993.

Žnidarič A, Denarie A, Richardson M, Woodward RJ. “SAMARIS Project – advanced materials for the rehabilitation of highway structures in Europe”. *Proceedings of the IABMAS Conference on Bridge Maintenance, Safety, Management and Cost*, United Kingdom: Taylor and Francis; 2005, p. 631-636.

Pakrashi V, O’ Connor A, Breysse D, Schoefs, F. “Reliability based assessment of structures in marine environment”. *Proceedings of the MEDACHS08 Conference on Construction Heritage in Coastal and Marine Environments*, 2005, Lisbon, CD-ROM.

Rouhan A, Schoefs F. “Probabilistic modelling of inspection results for offshore structures”. *Structural Safety*, vol. 25, 2003, p. 379 – 399.

Boukinda ML, Schoefs F, Quiniou-Ramos V, Birades M, Garretta R. “Marine growth colonization process in Guinea gulf: Data analysis”. *ASME Journal of Offshore Mechanics and Arctic Engineering*, vol. 129 no. 2, 2007, p. 97-106.

Itzhak D, Dinstein I, Zilberberg T. “Pitting corrosion evaluation by computer image processing”. *Corrosion Science*, vol. 21, 1981, p. 17-22.

Choi KY, Kim SS. “Morphological analysis and classification of types of surface corrosion damage by digital image processing”. *Corrosion Science*, vol. 47, 2005, p. 1-15.

Pakrashi V, Schoefs F, Memet JB, O’ Connor A. “ROC dependent event isolation method for image processing based assessment of corroded harbour structures”. *Journal of Structure and Infrastructure Engineering*, vol. 6 no. 3, 2010, p. 365-378.

Battiato S, Castriona A, Mancuso M. “High dynamic range imaging for digital still camera: an overview”. *Journal of Electronic Imaging*, vol. 12 no. 3, 2003, p. 459-469.

Jacobs K, Loscos C, Ward G. “Automatic high dynamic range image generation for dynamic scenes”. *IEEE Computer Graphics and Applications*, vol. 28 no. 2, 2008, p. 84-93.

Wandell BA, El Gamal A, Girod B. “Common principles of image acquisition systems and biological vision”. *Proceedings of the IEEE*, vol. 90 no. 1, p. 5-17.

Colbert M, Reinhard E, Hughes CE. “Painting in high dynamic range”. *Journal of Visual Communication and Image Representation*, vol. 18 no. 5, 2007, p. 387-396.

Pell D. *Shoot to thrill: A hard-boiled guide to digital photography*. 1st ed. Que Publishing; 2009.

Reinhard E, Ward G, Pattanaik S, Debevec P. *High dynamic range imaging: Acquisition, display and image-based lighting*. 1st ed. Morgan Kaufman 2005.

Debevec, P. E., and Malik, J. "Recovering high dynamic range radiance maps from photographs". *Proceedings of SIGGRAPH 97, Computer Graphics Proceedings, Annual Conference Series*, 1997, p. 369-378

Liang MT, Lan JJ. "Reliability analysis for the existing reinforced concrete pile corrosion of bridge substructure". *Cement and Concrete Research*, vol. 35, 2005, p.540-550.

Darmawan MS, Stewart MG. "Spatial time – dependent reliability analysis of corroding pretensioned prestressed concrete bridge girders". *Structural Safety*, vol. 29, 2007, p.16-31.

Shivaraj K, Balasubramaniam K, Krishnamurthy CV, Wadhwan R. "Ultrasonic circumferential guided wave for pitting – type corrosion imaging at inaccessible pipe-support locations". *ASME Journal of Pressure Vessel Technology*, vol. 130 no. 2, 2008, p. 021502-1 – 11.

Qingyuan W, Kawagoishi N, Chen Q, Pidaparti RM. "Evaluation of the probability distribution in pitting corrosion fatigue life in aircraft materials". *Acta Mechanica Sinica* vol. 19 no. 3, 2006, p. 247-252.

Sailer C. "Pitting corrosion costs printer dearly", *Deutscher Drucker*, vol. 24, 2007, p. 15-16.
Tsushima T, Ishii A, Ochi Y, Masaoka N, Matsusue H. "Corrosion inspection of steel tube inner wall". *IEEE/ASME international conference on advanced intelligent mechatronics '97.* Final program and abstracts (cat no. 97TH8298), 34.

Misiti M, Misiti Y, Oppenheim G, Poggi J-M. *Wavelet Toolbox For Use with MATLAB, User´s Guide, version 2*. The MathWorks, Inc. 2002.

Naccari F, Battiato S, Bruna A, Castorina A. "Natural scenes classification for color enhancement". *IEEE Transactions on Consumer Electronics*, vol. 51 no. 1, 2005, p. 234-239

McGill RJ, Tukey W, Larsen WA. "Variations of Boxplots". *The American* Statistici*an*, vol. 32 no. 1, 1978, p. 12–16.